PIT SLOPE MANUAL

supplement 2-5

STRUCTURAL GEOLOGY CASE HISTORY

This supplement has been prepared as part of the

PIT SLOPE PROJECT

of the
Mining Research Laboratories
Canada Centre for Mineral and Energy Technology
Energy, Mines and Resources Canada

MINERALS RESEARCH PROGRAM
MINING RESEARCH LABORATORIES
CANMET REPORT 77-24

Available by mail from:

Printing and Publishing
Supply and Services Canada,
Ottawa, Canada K1A 0S9

CANMET
Energy, Mines and Resources Canada,
555 Booth St.
Ottawa, Canada K1A 0G1

or through your bookseller.

Catalogue No. M38 14/2-1977-5 Price: Canada: $2.75
ISBN 0-660-00993-5 Other countries: $3.30

Price subject to change without notice.

En vente par la poste:

Imprimerie et Édition
Approvisionnements et Services Canada,
Ottawa, Canada K1A 0S9

CANMET
Énergie, Mines et Ressources Canada,
555, rue Booth
Ottawa, Canada K1A 0G1

ou chez votre libraire.

N° de catalogue M38 14/2-1977-5 Prix: Canada: $2.75
ISBN 0-660-00993-5 Autres Pays: $3.30

Prix sujet à changement sans avis préalable.

THE PIT SLOPE MANUAL

The Pit Slope Manual consists of ten chapters, published separately. Most chapters have supplements, also published separately. The ten chapters are:

1. Summary
2. Structural Geology
3. Mechanical Properties
4. Groundwater
5. Design
6. Mechanical Support
7. Perimeter Blasting
8. Monitoring
9. Waste Embankments
10. Environmental Planning

The chapters and supplements can be obtained from the Publications Distribution Office, CANMET, Energy, Mines and Resources Canada, 555 Booth Street, Ottawa, Ontario, K1A 0G1, Canada.

Reference to this supplement should be quoted as follows:

Martin, D., Piteau, D. and Herget, G. Pit Slope Manual Supplement 2-5 - Structural Geology Case History; CANMET (Canada Centre for Mineral and Energy Technology, formerly Mines Branch, Energy, Mines and Resources Canada), CANMET REPORT 77-24; 29 p; Dec. 1977.

SUMMARY

Geological mapping of an iron ore pit was carried out over a four month period in the summer of 1973. The bulk of the field work consisted of lithological classification, detailed line mapping of minor and major structural discontinuities with the Discodat System and plane table mapping of major structural discontinuities.

About 25,000 ft (7600 m) of detailed line mapping were carried out covering the northern and eastern sections of the pit. Only joints greater than 12 ft (4 m) in trace length were recorded.

Plane table mapping was done with a telescopic alidade and a large drafting table was set up at three strategic points in the pit where major structures could easily be seen. These were located by sighting on the intersections of the structures with the toe and crest of the pit slope benches, and plotting on the 1 in. = 50 ft (1:600) mine plan.

Geological controls, such as major faults and marked changes in lithology, were utilized as the basic criteria for selecting fourteen preliminary structural domains. Five final structural domains were determined by comparing the orientation of minor discontinuities. Four joint sets were described as to tracelength, spacing, waviness and groundwater occurrence.

The pit was divided into seven design sectors based on structural domains and straight slope segments. Within each design sector, kinematically possible modes of instability were identified with respect to the orientation of major discontinuities and joint sets.

This identified the following combinations of structural discontinuities to be critical for design in the various areas of the pit:

a. major faults and cross joints on the north side
b. foliation joints on the south side
c. longitudinal joints and cross joints on the east side of the pit.

THE PIT SLOPE MANUAL

The Pit Slope Manual consists of ten chapters, published separately. Most chapters have supplements, also published separately. The ten chapters are:

1. Summary
2. Structural Geology
3. Mechanical Properties
4. Groundwater
5. Design
6. Mechanical Support
7. Perimeter Blasting
8. Monitoring
9. Waste Embankments
10. Environmental Planning

The chapters and supplements can be obtained from the Publications Distribution Office, CANMET, Energy, Mines and Resources Canada, 555 Booth Street, Ottawa, Ontario, K1A 0G1, Canada.

Reference to this supplement should be quoted as follows:

Martin, D., Piteau, D. and Herget, G. Pit Slope Manual Supplement 2-5 - Structural Geology Case History; CANMET (Canada Centre for Mineral and Energy Technology, formerly Mines Branch, Energy, Mines and Resources Canada), CANMET REPORT 77-24; 29 p; Dec. 1977.

SUMMARY

Geological mapping of an iron ore pit was carried out over a four month period in the summer of 1973. The bulk of the field work consisted of lithological classification, detailed line mapping of minor and major structural discontinuities with the Discodat System and plane table mapping of major structural discontinuities.

About 25,000 ft (7600 m) of detailed line mapping were carried out covering the northern and eastern sections of the pit. Only joints greater than 12 ft (4 m) in trace length were recorded.

Plane table mapping was done with a telescopic alidade and a large drafting table was set up at three strategic points in the pit where major structures could easily be seen. These were located by sighting on the intersections of the structures with the toe and crest of the pit slope benches, and plotting on the 1 in. = 50 ft (1:600) mine plan.

Geological controls, such as major faults and marked changes in lithology, were utilized as the basic criteria for selecting fourteen preliminary structural domains. Five final structural domains were determined by comparing the orientation of minor discontinuities. Four joint sets were described as to tracelength, spacing, waviness and groundwater occurrence.

The pit was divided into seven design sectors based on structural domains and straight slope segments. Within each design sector, kinematically possible modes of instability were identified with respect to the orientation of major discontinuities and joint sets.

This identified the following combinations of structural discontinuities to be critical for design in the various areas of the pit:

a. major faults and cross joints on the north side
b. foliation joints on the south side
c. longitudinal joints and cross joints on the east side of the pit.

20 Unstable southwest nose area due to intersection of observation fault and southwest fault 29

TABLES

1 Summary of minor discontinuity properties 9
2 Set orientation on the hanging wall, west and east of central fault zone 12
3 Ranges of dip direction and dip for various sets 13
4 Orientation data of minor discontinuity sets A to D 14
5 Properties of minor discontinuity sets 15
6 Possible unstable wedges involving major geologic structures 22
7 Design sectors and potential instability 26

INTRODUCTION

1. A detailed investigation of the structural geology of the hanging wall side of the Hilton mine open pit was conducted to delineate areas which could become subject to possible stability problems as the mine was deepened.

2. Instability of slopes in hard rock occurs because of failure along structural discontinuities such as foliation, joints, geological contacts, faults, etc. The most important single factor in stability analysis and design of rock slopes is therefore to determine location, orientation and other significant properties of discontinuities in the slope.

3. The study involved analysis of major discontinuities and joints to define structural domain boundaries and joint sets. Design sectors were delineated where slope geometry and structural geology are similar. Parameters considered in the structural analysis included orientation, size, spacing, waviness, rock hardness, and groundwater flow. Consideration was given to genetic and age relationships and to the question of extrapolating geological information with depth.

REGIONAL GEOLOGY

4. The Hilton mine is situated in the Ottawa River low land which is underlain predominantly by Precambrian basement rocks, the oldest of which are gneisses, quartzites and limestones of the Grenville Series. The Grenville rocks have been intruded by acidic and basic rocks and are overlain in several areas by flat-lying Paleozoic limestones, shales and sandstones. Pleistocene formations consist of till, sand, gravel and marine clays.

5. Most of the Grenville rocks have well developed gneissosity which strikes predominantly northeast and dips steeply southeast. The formations appear tightly folded along northeast trending axes. The folds are regional and have been deformed by continued metamorphism and igneous intrusions (1). Folding is difficult to recognize in the areas of heavy overburden near the mine, but drag folds were seen in the limestone and in ore in the pit.

6. The Hilton orebody occurs in rock somewhat less metamorphosed than the usual Grenville rocks in the area but are the same as the rest of the Grenville Series. The eastward trend of the Bristol beds, quite different from the regional trend, indicates that they were in a place that was protected from the more intense metamorphism that affected the rest of the area (1).

PIT SITE LITHOLOGY

7. The Hilton orebody consists of lenses and beds of magnetite and associated gangue minerals in a sequence of highly faulted Grenville metasediments which have been intruded by granite and granodiorite, producing a complex geological setting. The intrusions caused contact metamorphism of the metasediments and altered some of the metasediments to amphibolite and amphibolite skarn, which in turn provided favourable sites for the deposition of ore from hydrothermal solutions.

8. The ore zone is about 500 ft (152 m) wide and 2500 ft (760 m) long. It is roughly tabular and is conformable with the enclosing metasedimentary rocks, striking approximately east-west and dipping 55°N. The ore zone narrows and appears to pinch out at either end of the deposit. Exploratory drilling information indicates that

the ore zone appears to be continuous along dip.

9. The complex lithological distribution and major structural features within the pit are illustrated in Fig 1. A geological section of the pit is given in Fig 2. Photo mosaics of both the north or hanging wall and south or footwall sides, which indicate both the lithological and structural nature of the pit, are shown in Fig 3.

GRENVILLE METASEDIMENTS

10. The Grenville metasediments at the mine are gneisses, schists, hornfels, crystalline quartzitic limestone, quartzite and amphibolite, amphibolitic limestone (skarn) and minor serpentine. The only reliable stratigraphic marker horizon in the pit is a massive 140 ft (42 m) thick quartzite unit which occurs about 60 to 100 ft (18 - 30 m) above the ore zone.

11. The metamorphic gneisses occur only in the hanging wall of the ore zone. Granite gneiss and granodiorite gneiss are found north of the Northwall fault. Quartz biotite gneiss is found north of the quartzite and is often mixed with hornfels.

12. Three types of schist occur in the pit. Quartzo-feldspathic schist is a medium-grained schist with a moderately developed schistosity produced by aligned biotite flakes. Mica schist on the other hand has a very well developed schistosity due to an abundance of micaceous minerals. Talc schist is found on the north wall near the Northwall fault east of F13.

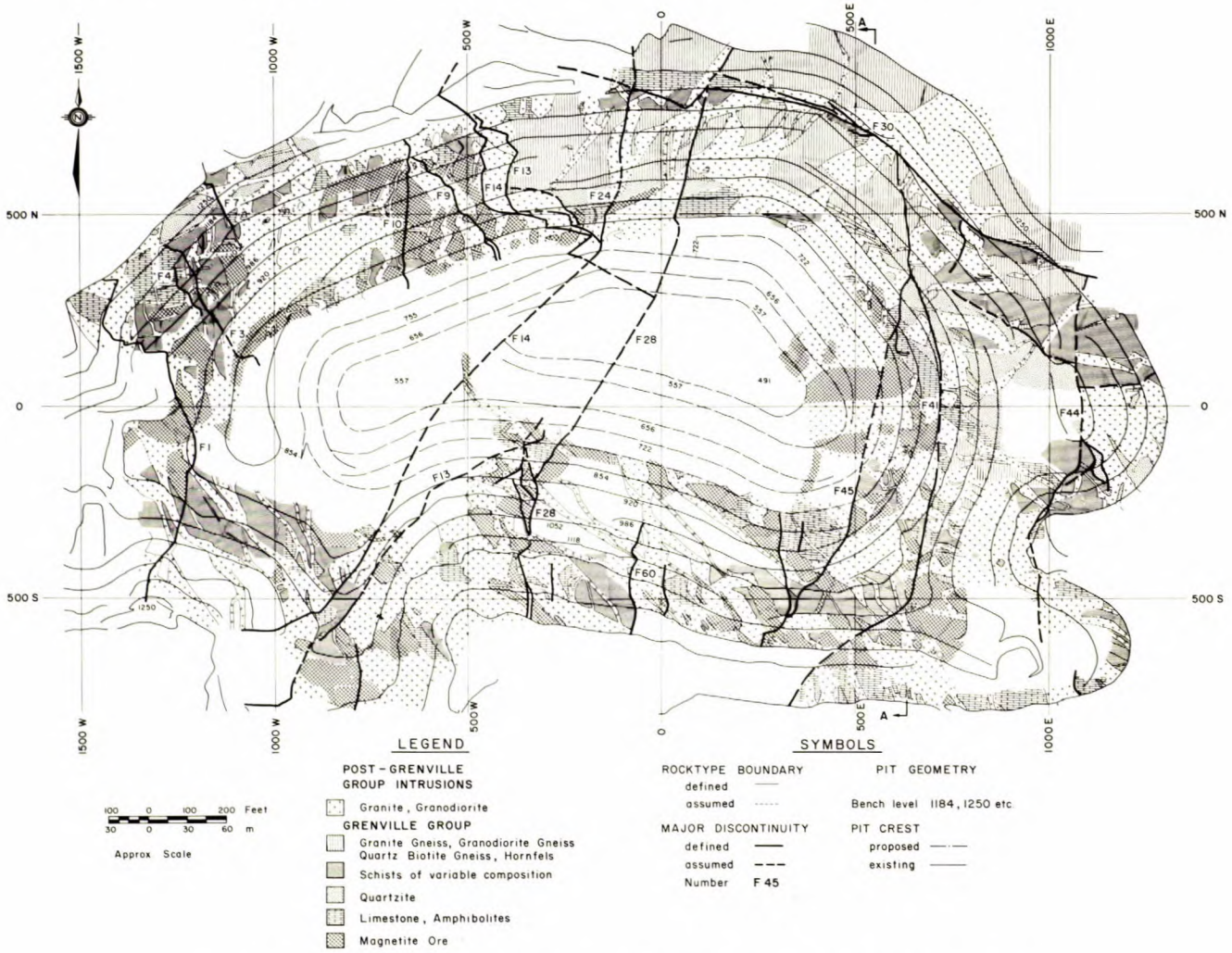

Fig 1 - Rock type distribution and major discontinuities of Hilton Mine pit.

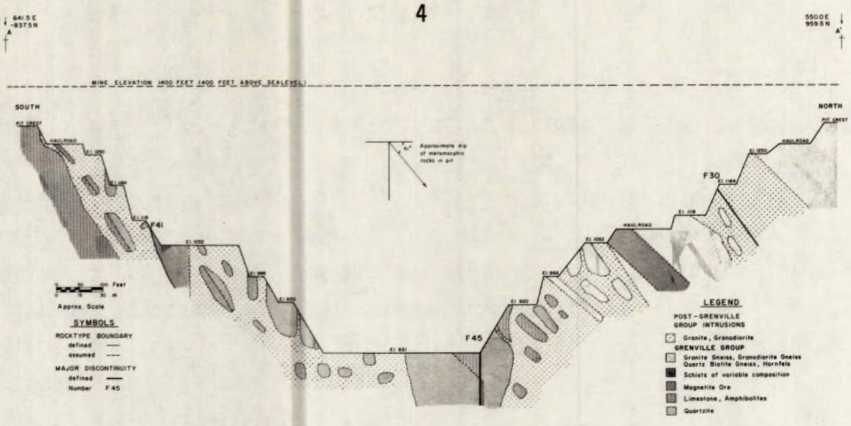

Fig 2 - Geological cross section of Hilton Mine.

13. Limestone in the footwall is massive, whereas in the hanging wall it consists of narrow distorted bands which grade into amphibolite, skarn, and/or ore.

14. Four types of amphibolite occur in the pit, three of which appear to have been formed by alteration of other Grenville rocks, mostly limestone. Massive hard coarse amphibolite and massive hard fine amphibolite are composed of green amphiboles (actinolite - tremolite), hornblende, and plagioclase. Minor minerals are magnetite and calcite. These amphibolites probably resulted from alteration of limestone. Amphibolite schist contains amphiboles and micas; their origin can probably be traced to alteration of carbonate rich schists. Light granular quartzose amphibolite is found with the quartzites. This rock is commonly found in the Grenville quartzite (1). Minor serpentinite is also evident in the pit. Serpentine commonly occurs with amphibolites in fault zones and on geological contacts.

INTRUSIVE ROCKS

15. Granite and granodiorite intrusions have completely dissected and possibly expanded the geologic section. Evidence suggests that these intrusive rocks provided the environment for ore deposition.

16. Granite is the most abundant intrusive rock and is exposed nearly everywhere within the pit boundary. These rocks weather differently from the host rock and cut across metamorphic units as sills, dikes, and lenses.

17. Granodiorite, being less abundant, appears to have essentially the same engineering properties as the granite and is either of the same age or slightly younger.

ORE ZONE ROCKS

18. Four types of ore in the pit are classified as massive coarse, banded, massive fine, and schistose, which appear to result from replacement of the amphibolized Grenville rocks.

19. Massive coarse ore is composed of magnetite, amphiboles and minor calcite and lacks any defined compositional layering. Banded ore has a composition similar to the massive coarse ore except for a distinct banding of magnetite and amphiboles. In some places, banded ore contains more calcium carbonate than magnetite or amphiboles due to only partial replacement of the pre-ore metasedimentary rocks. Massive fine ore is composed of fine grained magnetite and amphiboles and has very poorly developed compositional layering. Schistose ore is similar to banded ore except that it contains micas and platy amphiboles as accessory minerals.

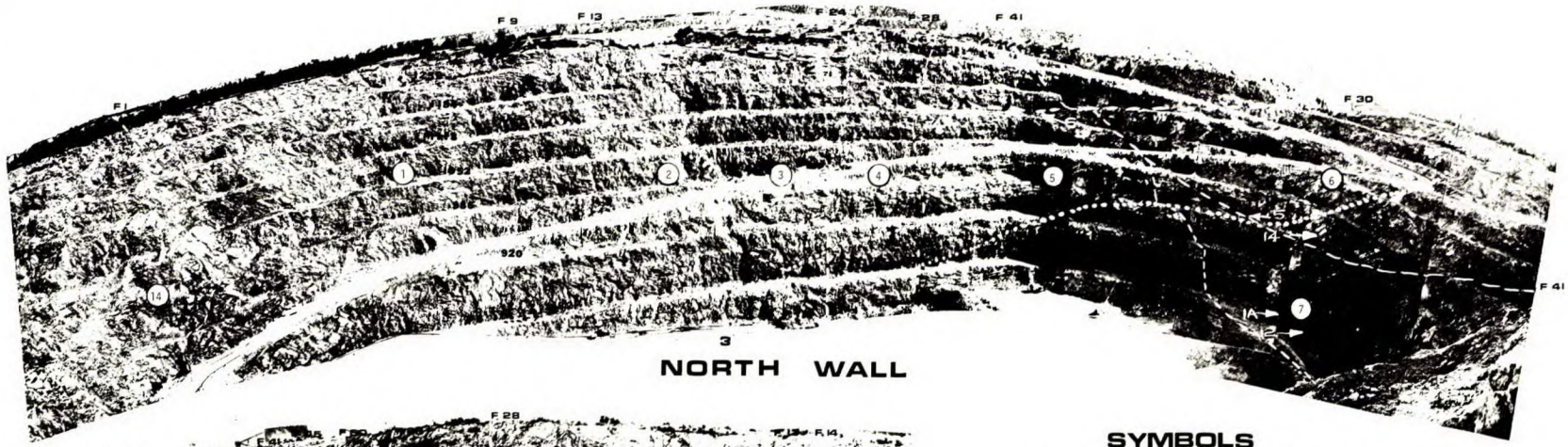

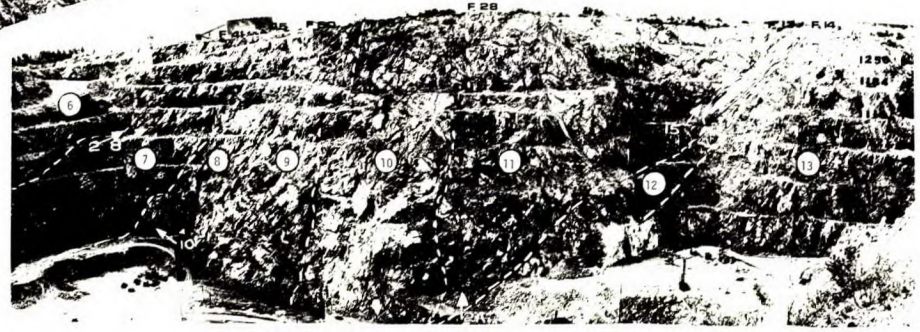

SYMBOLS

TRACE OF MAJOR FAULT DEFINING STRUCTURAL DOMAINS	F 28
FOOTWALL CONTACT OF QUARTZITE	
NUMBER OF STRUCTURAL DOMAIN	(5)
NUMBER, LOCATION AND DIRECTION OF PHOTOGRAPH	←15
BENCH ELEVATION	986

Fig 3 - Important structural features of Hilton Mine pit.

STRUCTURAL GEOLOGY OF PIT SITE

FAULTS

20. Faults extent in most cases over 100 ft (30 m) and are classified as major discontinuities. This means they are mapped individually and if critically orientated would cause sufficient concern to adjust the slope angles. The dominant set of faults and associated shears strike north-south and dip between 55 to 65 degrees to the east as indicated in Fig 1 and in the lower hemisphere of the equal area net of Fig 4(a). Another obvi-

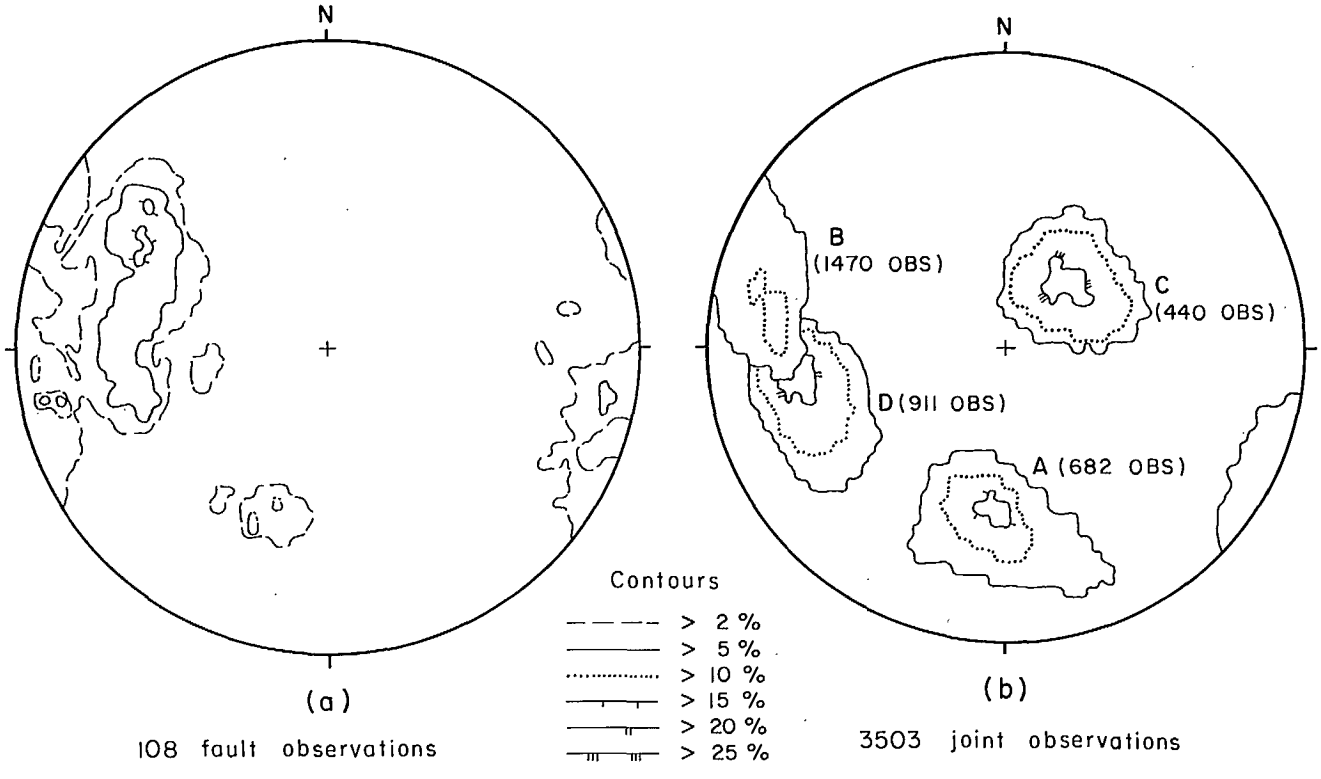

Fig 4 - Equal area net of lower hemisphere showing major faults (a) and joints (b) for pit area.

ous fault set occurs parallel to the compositional layering of the metasediments. Other faults not included above, although generally dipping steeply, appear to be distributed randomly. The majority of the major faults are shown in Fig 3.

21. The nature of fault material and width of the fault zones vary depending on the nature of the fault and the rock type. However, fault gouge commonly occurs as a soft white clay containing calcite stringers. Breccia material is generally dark green serpentine or altered wall rock with calcite stringers and mud. Other minerals found in fault zones are amphiboles, serpentine, talc, micas, magnetite, pyrite, hematite, quartz, and feldspar. Nearly all major faults have an abundant flow of water and contain very damp, moist material in the fault zone.

22. Faults have offset the granite and granodiorite, indicating that faulting is more recent than the youngest rocks. In most cases, the amount of offset is impossible to determine, but in some places appear to be several tens of feet. Offset ranges from 2 ft (0.6 m) on small faults to approximately 200 ft (60 m) on large faults. The East fault, no. 41 in Fig 1, for example, has a normal displacement of 20 ft (6 m) as indicated in Fig 5, whereas the Southwest fault, no. 13 in Fig 1, has displaced the orebody approximately 200 ft (60 m). The twisted and drag folded nature of the material adjacent to this fault is evident through the Central Fault Zone between fault no. 13 and fault no. 14.

23. The relationship between offsets of fault structures, indicate at least two stages of faulting for the area.

Fig 5 - East fault with a displacement of 20 ft (6 m).

SHEARS

24. Shears are analogous to minor faults and, at the Hilton mine, are considered for purposes of identification to be those structures containing striae and grooves, but which have nominal breakage and displacement. The general trends of shears mapped in the pit are similar to the faults.

COMPOSITIONAL LAYERING

25. Compositional layering occurs as gneissosity in gneisses, schistosity in schists and ore, bedding in limestone and quartzite, and as banding in ore rocks. Examples of compositional layering are seen in Fig 6.

26. Shown in Fig 7 is a plot of the strike of the compositional layering on both the hanging wall and footwall in the various preliminary structural subareas going from west to east across the pit. It can be seen that compositional layering rotates in a clockwise direction from west to east. The compositional layering rotates through

Fig 6 - Compositional layering.

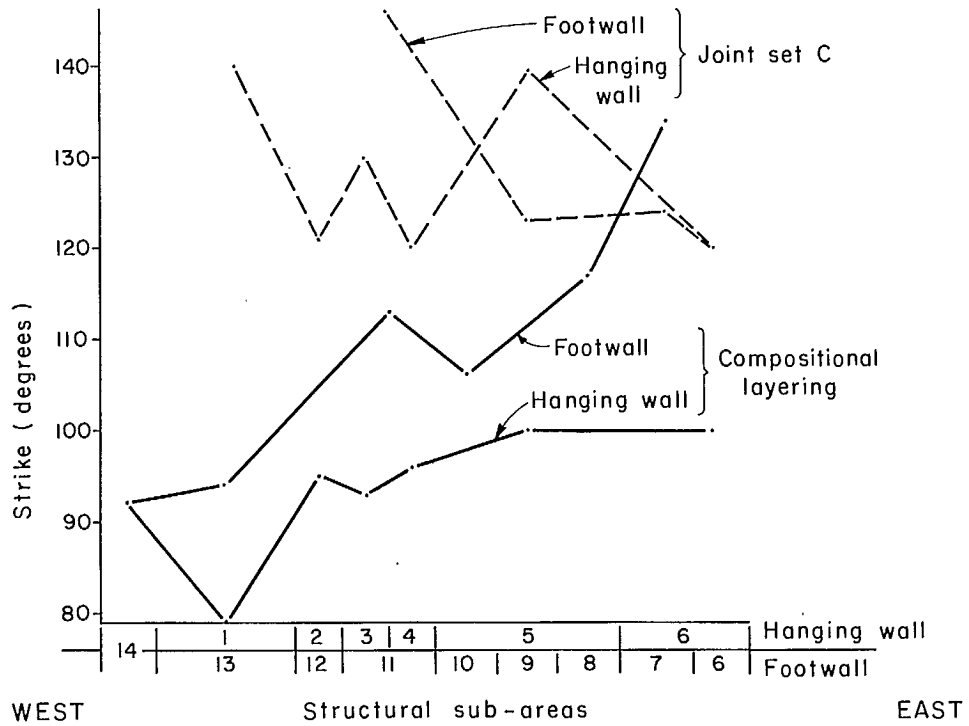

Fig 7 - Strike of compositional layering and set C.

about 40° going from a strike of 90° on the west side to about 130° on the east side of the pit.

27. Folding of compositional layering was mapped in ore and limestone, but the quantity and magnitude of minor folds were not sufficient to obtain a relationship to major folds in the area. Axial planes of minor folds, however, could be traced for as much as 3 ft (0.9 m) in some cases. Fractures parallel to compositional layering have pronounced undulations - as do several major faults, especially the Southwest fault.

GEOLOGICAL CONTACTS

28. Geological contacts occur between intrusive or metamorphic rocks or both. Contacts between metamorphic rocks are generally comformable with the compositional layering. Contacts of intrusive dykes have a general north-south trend and westerly dip varying from 20° to 70°.

29. Healed contacts are generally irregular and for engineering purposes appear relatively insignificant with respect to stability. On the other hand, open contacts are generally damp and contain infillings which vary depending on the type of wall rock. Serpentine and amphibole are common on all contacts. Other minerals found are calcite, mica, and pyrite.

30. The length of contacts varies considerably. Continuous contacts are prominent on the south wall where the host rock occurs as elongated lenses between extensive granite dykes. On the south wall, these contacts are important to stability of the slope. In a major wedge failure in 1972, for example, one such contact between granite and host rock formed one plane of the wedge.

MINOR DISCONTINUITIES

31. The term minor discontinuities has no genetical significance and comprises all relatively short and frequently occurring systematic fractures like joints (extension fractures) or shears or those following compositional layering. Minor discontinuities are described in regard to orientation, size, spacing, waviness, groundwater, and

wall rock hardness. A summary is given in Table 1.

Orientation

32. At first fourteen preliminary structural domains were chosen based on major faults and distinct changes in lithology. Measurements of orientation were carried out with a clino rule. A plot of all observations is given in Fig 4(b) which clearly shows the existence of four prominent sets as described below.

33. Set A: foliation fractures which consist of all fractures formed parallel to the compositional layering of the metamorphic rock sequence; this set is very dominant and has an average strike and dip of 093/55N throughout the pit.

34 Set B: cross joints which dip steeply, approximately normal to the hanging wall face and perpendicular to joint set C. These form angles between 70 and 77 degrees to the compositional layering and angles between 72 and 86 degrees to set C. The mean orientation of this set is 020/84E. The fractures of set B are generally not as continuous and appear to terminate at those of set C.

35. Set C: longitudinal fractures which dip moderately and form high angles with the compositional layering of set A and are approximately at right angles to the cross joints of set B. These fractures have an average attitude of 136/26SW. Due to their orientation they have resulted in some stability problems on the hanging wall and their orientations are independent of the 40° clockwise rotation of the metasediments from one side of the pit to the other.

36. Set D: these are fractures formed in association with faulting and shearing and appear to be the youngest in the pit. As they consist of shear and feather fractures, a wide range of orientations is to be expected. In comparing the equal area plots of the faults in Fig 4(a) and the minor discontinuities in Fig 4(b) it can be seen that the fractures conform with some of the main fault trends.

37. The vector mean orientation and the highest concentration in the cluster on the equal area net (peak) do not always agree. If a minor discontinuity set conforms to a spherical normal distribution or Fisher distribution, then the

Table 1: Summary of minor discontinuity properties

Sets	A	B	C	D
Orientation				
No. of obs.	682	1470	440	911
Peak concentration	094/46N	014/75E	130/25SW	171/60E
Fisher mean	093/55N	020/84E	136/26SW	165/59E
95% confidence (°)	1.3	1.0	1.1	0.9
99% confidence (°)	1.7	1.3	1.4	1.1
R/N	0.94108	D.94642	0.97317	0.96614
K	16.9	13.6	37.2	9.5
Spacing (ft)				
No. of obs.	386	1072	253	594
Mean (ft)	5.4	7.0	3.5	6.9
Standard dev.	6.3	7.4	3.2	7.1
Waviness				
No. of obs.	162	326	66	180
Mean ILA°	167	169	169	173
Standard dev.	8.4	7.6	5.9	7.8
Groundwater				
No. of obs.	682	1466	438	907
Most frequent class	3.5	3.8	3.9	4.0
Hardness				
No. of obs.	682	1470	440	911
Most frequent hardness	3.9	4.1	4.0	4.0
Standard dev.	0.6	0.6	0.6	0.6

Size in feet	Number of observations per minor discontinuity set			
	A	B	C	D
2 ft - 6 ft	1	3	0	1
6 ft - 20 ft	27	43	6	24
20 ft - 6D ft	644	1400	424	870
60 ft - 200 ft	8	21	8	11
Total	680	1467	438	906

vector mean of the distribution should correspond to the peak concentration, ie, the distribution centre on the net, and the density contour lines should be uniform about the mean. Lack of data and sampling bias and poorly defined population boundaries allow in most cases only a close approximation.

38. By rotating the mean of the discontinuity set to the centre of the equal area net and maintaining other portions of the distribution in their relative positions, ie, by rotating along small circles of the net, a representation of the set can be obtained which is not affected by distortion of the equal area net and a judgement is possible as to the fit of a spherical normal distribution. In the numerical analysis, the "Fisher" mean of the vectors was used for rotation to the centre of the net. The replotted joint sets are shown in Fig 8.

39. Some skewness of the discontinuity sets is evident in sets A, B and D, whereas set C is relatively conformable with the expected concentric

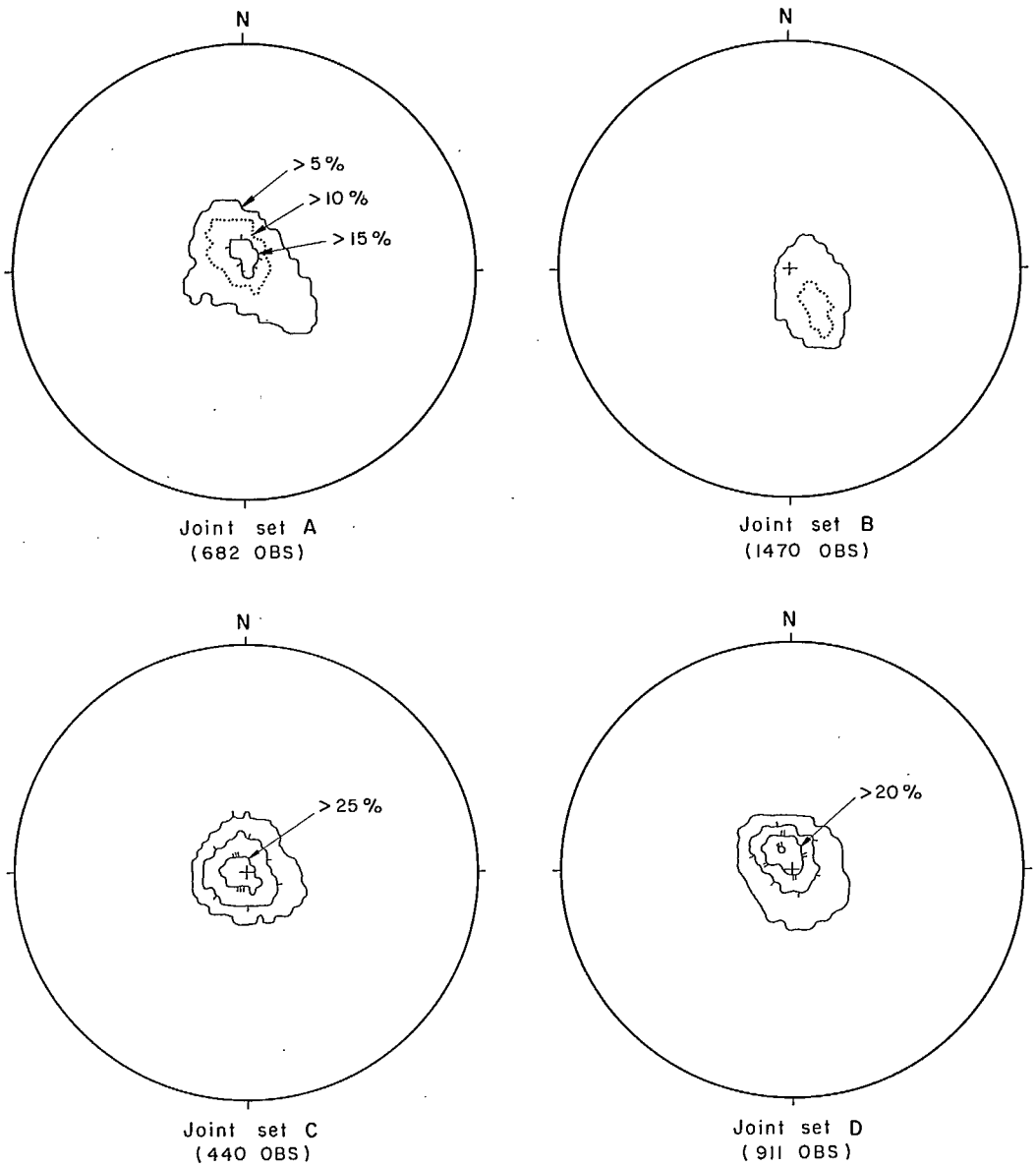

Fig 8 - Fisher mean and mode of joint sets in the pit area.

distribution. Skewness can possibly be explained as follows:

a. The effect on set A of minor folding and rolling of the foliation is evident throughout the pit;
b. Maxima B and D probably consist of sub sets (B1 and B2) and (D1 and D2) due to anisotropy and different strength properties of the metamorphic rocks compared with the intrusive rocks.
c. Uncertainty of distribution boundaries of the sets due to the overlap between sets B and D;
d. Directional bias of measurements taken in the field;
e. Discontinuity distributions may not fit the rotationally symmetric Fisher Distribution and a better fit may possibly be obtained with other distributions.

Lithological Control of Minor Discontinuity Orientation

40. To determine the lithological control of the orientation of minor discontinuities with respect to the metamorphic and intrusive rocks in the pit, separate equal area projections of fractures occurring in these rocks were compared in each of the 14 preliminary structural domains.

41. The results indicated that in some instances there are small differences between the means that occur in the metamorphic rocks and those occurring in the instrusive materials. Fractures of set A, ie, those parallel to the compositional layering, are about 10° steeper in the intrusive rocks than in the metamorphics. This variation in orientation is probably due to the anisotropy resulting from the compositional layering in the metamorphic rocks. Similar variations are also noted in sets B and D.

Variation of Minor Discontinuity Orientation with Depth

42. For purposes of evaluating variations of fracture orientations that may exist from the top to the bottom of the pit on the hanging wall, those fractures on the west side of the Central Fault Zone were compared with those on the east side. For the individual bench levels, preliminary structural domains 1 and 2 were combined on the west side and 3, 4 and 5 on the east side. Details concerning orientation and number of observations for sets A, C and D are given in Table 2.

43. The results indicate no obvious pattern of rotation with regard to either strike or dip of any of the sets in going from the top to the bottom of the pit.

44. However, with respect to the degree of development of the sets, it appears that set C is better developed on the east side of the Central Fault Zone than on the west side. If one assumes that variation in minor discontinuity frequency is due to changes in lithology, certain useful correlations can be made which might indicate structure at depth.

45. As the downthrow of 200 ft (60 m) of the Central Fault Zone is to the east, it would appear that joints below the existing benches mapped on the east side of the pit, will be similar to those already exposed and mapped on the west side. In other words, the average frequency of set C, which is unfavourably oriented with respect to stability, should decrease on the east side.

Dip Variation of Set C in the Hanging Wall

46. Figure 9 is a plot of the average dip of set C in the various preliminary structural domains in the hanging wall. It can be seen that the average dip is greater by about 15° in preliminary domains 2, 3 and 4 compared with preliminary domains 1, 5 and 6. These results would indicate why set C has tended to contribute to stability problems in the hanging wall slope in preliminary structural domains 2, 3 and 4.

Local Minor Discontinuities

47. The compilation of all measurements of minor discontinuities into one plot was useful for a general overview of the pit site. But this ignored significant differences and the previously selected 14 preliminary structural domains were grouped into five final structural domains. The limits of each set within each domain were defined on the equal area net by a range in dip direction

Table 2: Set orientation on the hanging wall, west and east of central fault zone

	Preliminary structural domains 1+2 (west side of pit)					Preliminary structural domains 3, 4, 5 (east side of pit)		
Bench level	Obs	Set A	Set C	Set D	Obs	Set A	Set C	Set D
1250					46	088/44N(6)	(-)	161/64E(10)
1118	201	086/51N(3)	141/20SW(2)	165/55E(11)	162	097/46N(2)	147/45SW(2)	172/60E(6)
1052	199	081/46N(4)	140/28SW(3)	156/54E(9)	267	(-)	170/20W(4)	170/63E(9)
986	189	090/47N(4)	147/25SW(2)	173/54E(10)	262	62/54N(2)	143/24SW(6)	172/59E(8)
920	183	066/48N(3)	123/48SW(2)	165/55E(12)				
821	198	091/47N(4)	130/37SW(1)	168/52E(8)	177	096/57N(5)	151/30SW(6)	16B/65E(7)
755	94	097/46N(4)	153/17SW(2)	175/62E(7)				

200' (61 m)

Note: 1) Set A: fracture set developed parallel to compositional layering of metasediments.
Set C: moderately dipping cross fractures approximately parallel to hanging wall and dipping toward pit.
Set D: steeply dipping fractures associated with shearing and faulting trends.

2) Fracture set orientations given as strike, dip and general direction of dip (eg, E = east); the number in parentheses ( ) indicates the peak concentration of the population in the equal area net.

3) (-) implies no fractures of the set were mapped in that structural domain.

4) No entry indicates an inaccessible bench.

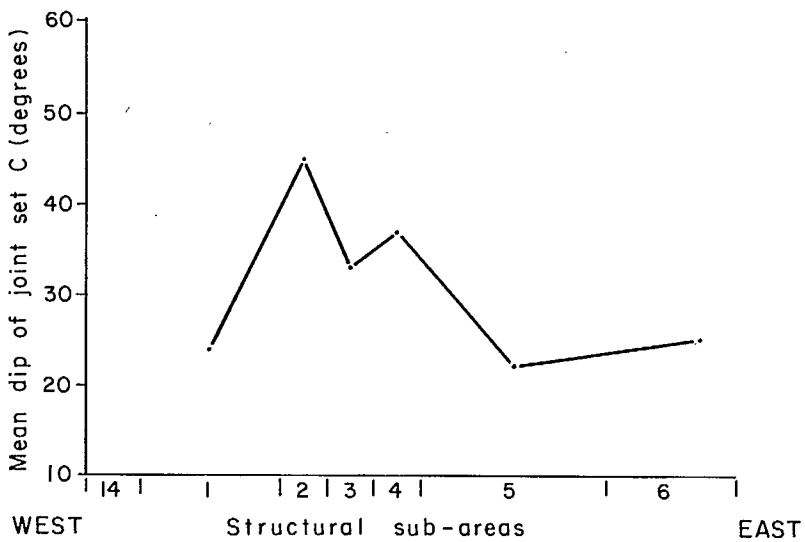

Fig 9 - Dip variation of joint set C in the hanging wall.

and dip. Because sets B and D occur close together on the net, it was not possible to define the exact boundary between them, and some overlap resulted. This overlap may have skewed the distributions. The limits of the sets are shown in Table 3.

48. The five structural domains are shown on Fig 10 and comprise the following preliminary

Table 3: Ranges of dip direction and dip for various sets

Final domains	Preliminary domains	Set A Dip direction	Set A Dip	Set B Dip direction	Set B Dip	Set C Dip direction	Set C Dip	Set D Dip direction	Set D Dip
	All observations	332°-360° 0°-33°	30°-82°	84°-144° 264°-324°	60°-90° 60°-90°	180°-270°	6°-45°	45°-96°	36°-76°
D1	1,2	332°-360° 0°-24°	28°-88°	89°-134° 266°-320°	65°-90° 58°-90°	186°-246°	4°-60°	35°-89°	12°-74°
D2	3,4,5	337°-360° 0°-18°	36°-72°	91°-158° 260°-336°	70°-90° 60°-90°	192°-298°	0°-40°	26°-114°	30°-76°
D3	6,7	345°-360° 0°-52°	19°-71°	98°-163° 277°-338°	78°-90° 65°-90°	176°-284°	4°-56°	68°-120°	42°-80°
D4	8,9,10,11	328°-360° 0°-52°	20°-80°	98°-159° 273°-319°	76°-90° 66°-90°	167°-249°	10°-60°	63°-119°	26°-76°
D5	12,13,14	320°-360° 0°-31°	28°-80°	97°-154° 262°-315°	56°-90° 70°-90°	-	-	42°-97°	38°-80°

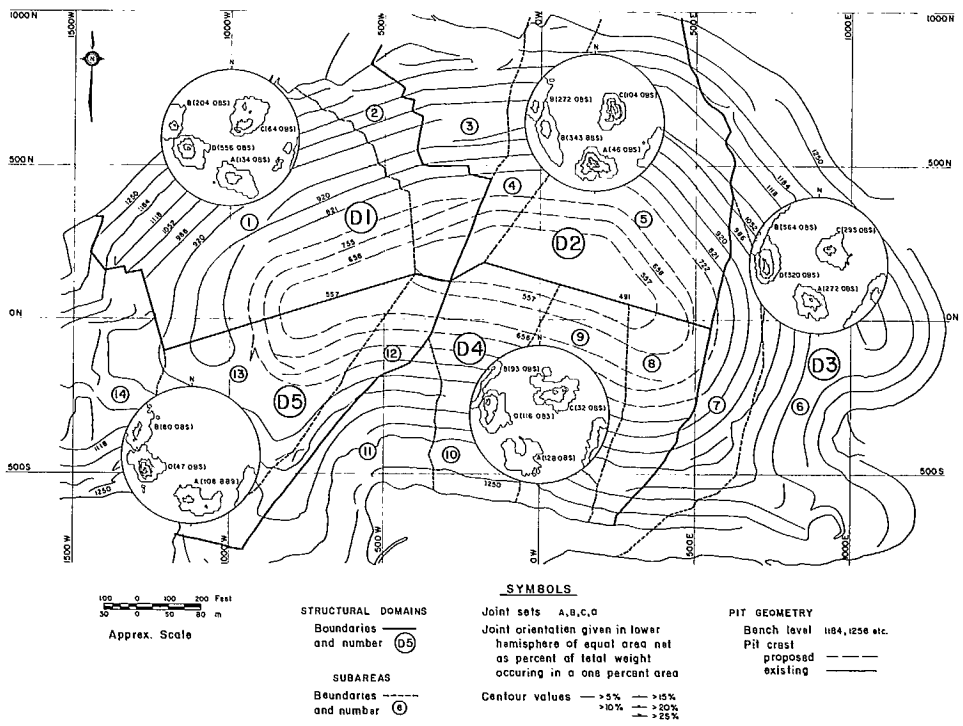

Fig 10 - Structural domains and orientation of joint sets of Hilton Mine pit.

structural domains:

Final Domains	Preliminary Domains
D1	1,2
D2	3,4,5
D3	6,7
D4	8,9,10,11
D5	12,13,14

Orientation in Final Domains

49. The orientation of minor discontinuity sets was examined for each domain. Equal area plots of sets in each domain are shown in Fig 10 and orientation data are summarized in Table 4. The analysis was carried out assuming that the sets fit a spherical normal distribution or Fisher distribution. The vector mean of orientation, confidence limits of the mean, and dispersion parameters for each set are given. Descriptions of the properties of the spherical normal distribution are given in the main text of the structural chapter.

Size

50. It can be seen in Table 1 and the more detailed Table 5 that most minor discontinuities mapped are between 20 and 60 ft (6 - 20 m) in length, ie, less than one bench height. Since only fractures greater than 12 ft (3.6 m) were mapped, a complete sample of the range of sizes was not obtained and no attempt was made to carry out an analysis on the basis of a negative normal

Table 4: Orientation data of minor discontinuity sets A to D

Set	Domain	Number of obs.	Peak orientation Strike	Dip	Mean orientation of Fisher distribution Strike	Dip	Variation of Fisher mean (°) 95% confidence	99% confidence	Resultant vector / observations (R/N)	Concentration parameter (K)
	D1	134	088	51N	084.9	57.2N	2.9	3.7	.94518	18.1
	D2	46	094	49N	089.7	54.4N	3.6	4.5	.97240	35.4
	D3	272	101	43N	104.8	50.1N	2.0	2.4	.95041	20.0
	D4	128	098	40N	107.6	57.5N	3.5	4.4	.92648	13.5
A			114	65N						
	D5	106	094	56N	082.8	58.1N	3.5	4.3	.93977	16.4
	All observations of set A	682	094	46N	093.2	55.4N	1.3	1.7	.94108	16.9
	D1	204	012	72E	009.1	56.0E	11.4	14.1	.93123	1.7
	D2	272	016	80E	025.9	89.5E	2.2	2.7	.93744	15.9
B	D3	364	D27	88W	033.9	85.5W	1.8	2.2	.94611	18.5
	D4	93	024	90	026.7	88.5W	3.1	3.9	.95748	23.3
	D5	80	023	76E	027.4	82.1E	4.0	4.9	.94171	16.9
	All observations of set B	1470	D14	75E	20.0	84.3E	1.0	1.3	.94642	13.6
	D1	64	133	21SW	127.4	34.1SW	3.9	4.9	.95434	21.6
	D2	104	158	30W	148.4	24.8W	2.2	2.7	.97641	42.0
C	D3	293	121	25SW	136.8	26.3SW	1.6	2.0	.96341	27.2
	D4	32	122	33SW	123.9	34.6SW	5.6	7.0	.95508	21.6
	D5	-	-	-	-	-	-	-	-	-
	All observations of set C	440	130	25SW	136.3	26.1SW	1.1	1.4	.97317	37.2
	D1	356	164	54E	158.7	51.1E	1.6	2.0	.95354	21.5
	D2	343	174	62E	165.7	60.3E	2.0	2.4	.93742	15.9
D	D3	320	176	65E	004.3	56.4E	1.4	1.8	.96754	30.7
	D4	116	167	66E	004.7	56.9E	2.6	3.3	.96185	26.0
	D5	47	160	62E	163.8	58.5E	4.2	5.2	.96188	25.7
	All observations of set D	911	171	60E	165.3	59.1E	0.9	1.1	.96614	9.5

Table 5: Properties of minor discontinuity sets

Set	Domain	No. of obs.	No. of observations fracture size (ft) 2-6	6-20	20-60	60-200	Spacings No. of obs.	Mean space (ft)	S.D.*	Waviness No. of obs.	Mean interlimb angle (°)	S.D. of interlimb angle	Groundwater No. of obs.	Mean	S.D.	Hardness No. of obs.	Mean	S.D.
	D1	134	0	5	128	1	71	4.3	6.6	44	168	7.6	134	3.7	.80	134	R3.8	.67
A	D2	46	0	0	43	3	18	4.9	5.0	12	169	7.3	46	4.1	1.11	46	R3.9	.61
	D3	266	0	2	263	1	158	5.3	5.7	55	168	9.2	272	3.6	.89	272	R3.8	.63
	D4	128	1	7	120	0	81	6.4	7.0	23	165	9.1	128	3.1	.53	128	R4.1	.67
	D5	106	0	7	97	2	73	4.8	5.7	23	165	10.1	106	3.1	.72	106	R3.9	.61
	All set A	680	1	27	644	8	386	5.4	6.3	162	167	8.4	682	3.5	.89	682	R3.9	.64
	D1	204	0	12	191	1	127	8.8	8.9	54	168	7.6	204	4.0	.97	204	R4.1	.53
B	D2	272	0	8	261	3	191	7.4	6.9	66	169	7.6	272	4.2	.97	272	R4.2	.53
	D3	364	0	3	354	7	238	7.4	7.6	69	169	7.1	363	3.6	.98	364	R4.0	.58
	D4	93	0	6	86	1	49	8.7	9.2	16	167	3.3	93	3.1	.47	93	R4.1	.58
	D5	79	0	8	71	0	60	6.8	8.7	17	174	5.1	79	2.9	.36	80	R4.0	.54
	All set B	1467	3	43	1400	21	1072	7.0	7.4	326	169	7.6	1466	3.8	1.0	1470	R4.1	.58
	D1	64	0	2	61	1	22	7.2	5.7	11	165	5.8	64	3.9	.88	64	R3.9	.64
C	D2	105	0	1	99	4	65	3.2	2.8	8	173	6.2	104	4.3	.81	104	R4.1	.36
	D3	290	0	4	282	4	189	3.5	3.3	46	170	4.9	291	3.7	.89	293	R4.0	.62
	D4	32	0	2	30	0	11	5.0	6.2	5	174	8.2	32	3.3	.87	32	R4.4	.56
	D5	-	-	-	-	-	-	-	-	-	-	-	-	-	-	-	-	-
	All set C	438	0	6	424	8	253	3.5	3.2	66	169	5.9	438	3.9	.89	440	R4.0	.57
	D1	345	1	16	324	4	267	6.1	6.4	59	171	8.1	356	4.0	.95	356	R4.0	.61
D	D2	339	0	4	329	6	256	6.3	6.4	88	172	8.0	342	4.3	.94	343	R4.1	.53
	D3	318	0	2	312	4	192	7.0	6.3	75	170	8.4	317	3.7	1.01	320	R3.9	.60
	D4	116	2	2	112	0	68	6.8	8.3	16	167	7.8	116	3.3	.64	116	R4.1	.59
	D5	47	0	3	44	0	22	4.2	4.2	10	171	5.5	46	3.2	.91	47	R3.8	.45
	All set D	906	1	24	870	11	594	6.9	7.1	180	173	7.8	907	4.0	.98	911	R4.0	.58

*S.D. = standard deviation

distribution.

51. A clear distinction between the average size of minor discontinuities in each set was not possible. Field observation indicated that discontinuities of set A and D tend to be well developed and generally longer than those of sets B and C. In general, fractures of set B were observed to be shorter than those of set C.

Spacing

52. The mean and standard deviations for spacing are shown for each set in Table 1 and Table 5 based on the negative exponential distribution.

53. The standard deviations of the mean are quite high due to the possible large error introduced by correcting for bearing of the traverses in relationship to strike of the minor discontinuities. An example is given in Fig 11 for set A.

Waviness

54. Measurements of waviness angles were plotted in histograms as shown in Fig 12. Mean and standard deviations of interlimb angles for the four sets are given in Table 1.

55. Waviness was only measured for about 20 per cent of the mapped discontinuities. Those for which it was not measured were either irregular or inaccessible.

56. Variations in the average waviness of sets in different zones may be related to different quality of exposures. Fractures of set A are much better exposed in domains D4 and D5, and accordingly the waviness is much better defined in

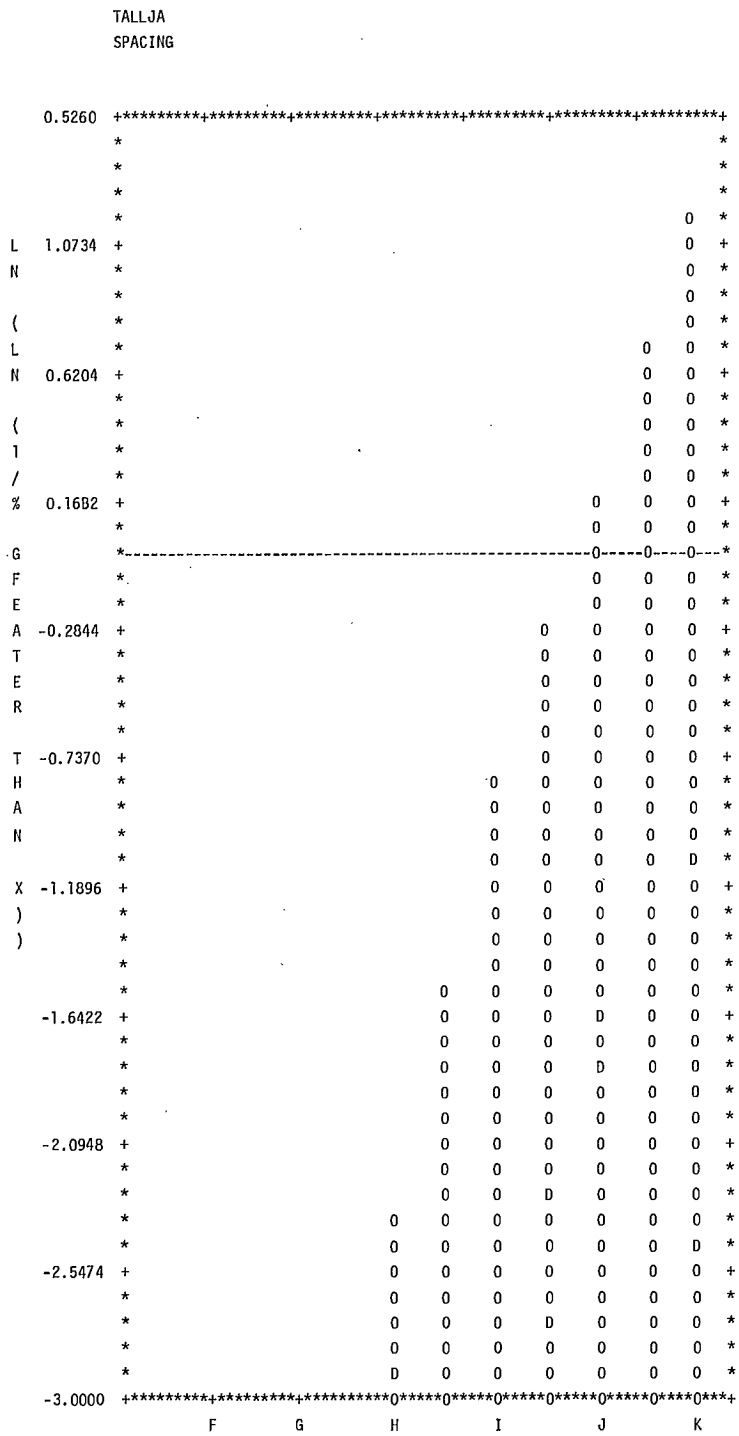

TOTAL NO. OF DISCONTINUITIES = 682
FREQUENCY TABLE FOR VARIABLE SPACING
TOTAL NO. OF OBSERVATIONS = 386

	X	NO. LESS THAN	% LESS THAN X
F	0.6	0.	0.0
	1.1	0.	0.0
G	2.0	6.	1.55
	3.5	15.	3.89
H	6.0	36.	9.33
	11.0	77.	18.39
I	20.0	135.	34.97
	35.0	205.	53.11
J	60.0	270.	69.95
	110.0	338.	87.56
K	200.0	369.	95.60
	350.0	384.	99.48
L	600.0	386.	100.00
	1100.0	386.	100.00
M	2000.0	386.	100.00

MEAN SPACING (1/LAMBDA) = 54.21

TEST OF HOMOGENEITY OF SPACINGS F = 379.40
HAS CHI-SQUARED DISTRIBUTION WITH 385 DEGREES OF FREEDOM

MEAN OF OBSERVED SPACINGS IS 54.21
STANDARD DEVIATION OF OBSERVED SPACINGS IS 63.38
MEAN OF LOGARITHMS OF OBSERVED SPACINGS IS 3.42
STANDARD DEVIATION OF LOGARITHMS OF OBSERVED SPACINGS IS 1.14
11:28:15 2.081 RC=0
SI PREVIOUS

CHISQUARED TABLE FOR Z
LOG (Z) = LAMBDA*X, WHERE
LAMBDA = 1/MEAN SPACING
X = SPACING

CLASS LIMITS	FE	FO	(FE-FO)**2/FE
0.0 - 1.33	97.	100.	0.1
1.33 - 2.00	97.	115.	3.5
2.00 - 4.00	97.	89.	0.6
4.00 OVER	97.	82.	2.2

CHISQUARED = 6.44

Fig 11 - Spacing plot of joint set A.

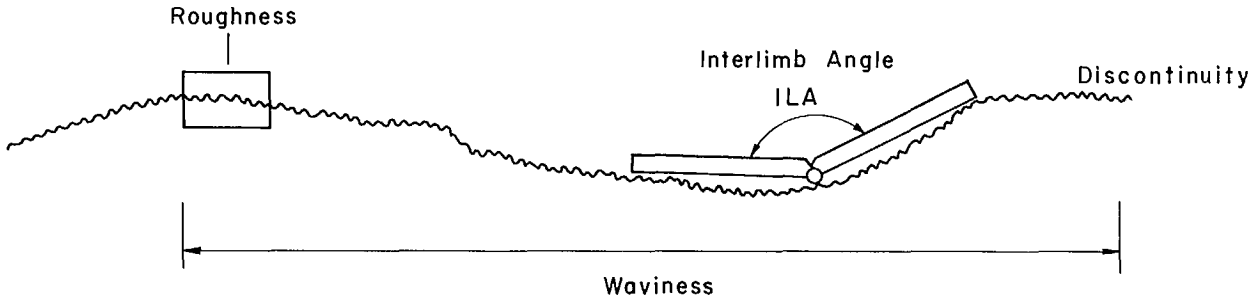

TALLJA

HISTOGRAM 3 - (180-ILA)/2

Frequency	19	0	2	3	4	4	6	3	8	11	12	6	4	4	11	11	5	4	4	1
Each * equals	1 points																			
19	*																			
18	*																			
17	*																			
16	*																			
15	*																			
14	*																			
13	*																			
12	*										*									
11	*									*	*				*	*				
10	*									*	*				*	*				
9	*									*	*				*	*				
8	*								*	*	*				*	*				
7	*								*	*	*				*	*				
6	*						*		*	*	*	*			*	*				
5	*						*		*	*	*	*			*	*	*			
4	*				*	*	*		*	*	*	*	*	*	*	*	*	*	*	
3	*			*	*	*	*	*	*	*	*	*	*	*	*	*	*	*	*	
2	*		*	*	*	*	*	*	*	*	*	*	*	*	*	*	*	*	*	
1	*		*	*	*	*	*	*	*	*	*	*	*	*	*	*	*	*	*	*
Interval	.0	.5	1.0	1.5	2.0	2.5	3.0	3.5	4.0	4.5	5.0	5.5	6.0	6.5	7.0	7.5	8.0	8.5	9.0	9.5
Class																				

Mean = 6.4 St. Dev. = 4.22 No. of observations = 162 No. of discontinuities = 682

↑

field dilatancy (d_o)

Fig 12 - Histogram of waviness measurements of joint set A.

these areas. It is generally noted that older sets have smoother waves than those more recently formed.

Groundwater

57. All minor discontinuity sets in the pit show evidence of water flow. The mean flow for each set is summarized in Table 1. It generally appears that set D has a greater flow than the others.

58. It was noted that there was more water along joints in the hanging wall. The reason appears to be that the natural drainage in the pit occurs along well developed foliation joints which seldom daylight on the footwall side. Major traverse faults on the hanging wall, however, carry abundant water as do fractures of set D parallel to these faults.

Hardness

59. As might be expected, hardness of the fracture walls is relatively uniform for all sets. As shown in Table 1, the mean hardness is about R4. The uniform distribution of hardness for all sets indicates that no alteration or other effects have accompanied the formation of the discontinuity sets in the pit. An example is shown in Fig 13.

SUMMARY OF GEOLOGICAL EVOLUTION

60. The general geological evolution and structural history of Hilton mine rocks appears to have involved the following stages which are discussed in chronological order:

i. Deposition of a flat-lying sedimentary sequence of argillaceous material, ie, shale, siltstone, etc, arenaceous material, ie, sandstone, etc, and calcareous materials.

ii. Low to medium grade metamorphism and the folding of the strata into a steeply dipping sequence. Until this time, all deformation was by and plastic flow followed by recrystallization.

iii. Granite and granodiorite intrusions spread over two phases. Doming during the intrusive phases appears to have caused additional deformation of the metasediments as indicated by the general clockwise rotation of the compositional layering from west to east across the pit, set A. This doming of the metasediments must have occurred before the cross fractures, set B, and longitudinal fractures, set C, were developed because these sets do not rotate as does the compositional layering.

iv. Subsequent to metamorphism and intrusion was the development of sets A, B, and C and the majority of faults. Set D developed in connection with the transverse faults which maintain a position approximately at right angles to the strike of the compositional layering.

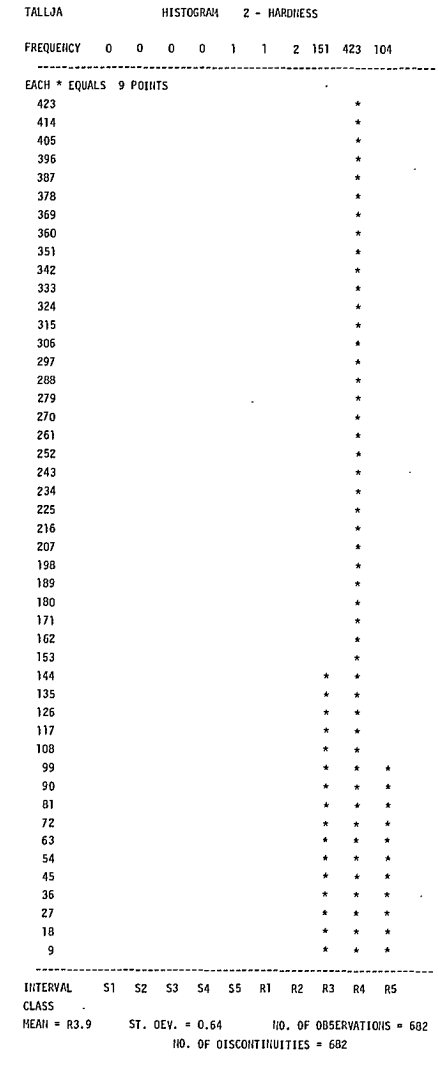

Fig 13 - Histogram of hardness measurements of joint set A.

GROUNDWATER

61. The groundwater table appears to be near the excavation surface in the hanging wall and water is apparent on nearly all benches. Seepage generally starts about 15 ft (4.5 m) below the crest of each bench with the result that bench faces are generally wet from that point down to the toe. The possible groundwater level in the hanging wall is indicated in Fig 14.

62. A large amount of groundwater infiltration may be due to near surface drainage of a diverted stream and swamp land located behind the crest of the pit. These areas are partly filled all year due to frequent rain, the average rainfall being about 36 in. (0.9 m) per year. The stream on the north side of the pit is in the gully near the Northwall faults. Significant seepage occurs along this fault on bench 1184N and 1118N. This stream is dammed about 250 ft (75 m) from the pit crest and water is pumped along the top of the north wall into the gully on the east side of the pit.

63. The most abundant water flow in the pit is along major faults. Faults generally appear to be permeable, especially in the lower reaches where free running water is evident. Open joints or contacts occasionally show similar freely running water conditions, although the quantity is generally less.

64. It appears that groundwater problems develop during the winter and spring when ice tends to retard free drainage of the slope. Also, frost action can also lead to numerous rock falls. It is significant that the Central Fault Zone is so highly fractured that it appears to be almost entirely free draining. In comparison with adjacent wall rock, this zone contains no damp or wet spots.

Summary of Groundwater Occurence in Joints

Damain	Location	Average Water Classification for All Joints in Zone
D1	West Hanging Wall	3.96
D2	East Hanging Wall	4.29
D3	East Wall	3.76
D4	East Footwall	3.14
D5	West Footwall	3.83

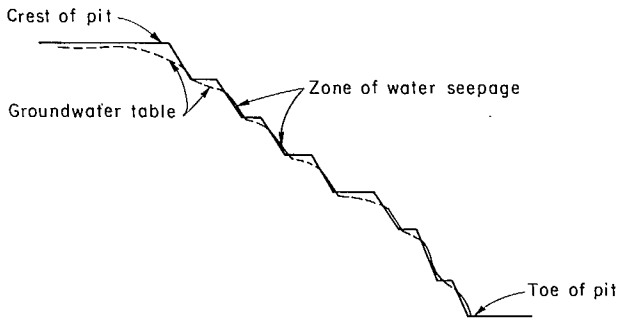

Fig 14 - Groundwater level in the hanging wall, with a visual classification of seepage.

KINEMATIC ANALYSES

65. An analysis was carried out to determine individual or combinations of discontinuities which could possibly lead to slope instability as the pit was deepened. Both overall slope failure and bench failure were considered. The following instability modes were examined: plane shear, stepped plane shear, 3-d-wedge, and blockflow.

ANALYSIS OF MAJOR DISCONTINUITIES

66. All discontinuities which could be traced for more than two bench heights or 120 ft (36 m) are considered to be major structures and all 75 major discontinuities observed were analyzed. Judgement was required in assigning an attitude to some structures which may have been mapped in several different localities in the pit.

67. Major discontinuities are most often involved in wedge instability. Before being considered as potentially unstable, wedges involving major structures must satisfy all the following requirements (Fig 15):

a. The two planes that form a wedge must have an interior dihedral angle of less than 180° and, except for planes within ± 5° of vertical, must dip in opposite directions;
b. The line of intersection must plunge between 20° and 60° in the direction of dip of the pit: wedge intersections with plunge less than 20° are considered stable and those greater than 60° are steeper than the overall pit slope angle;
c. The azimuth of the line of intersection must be within ± 15° of the direction of dip of the slope; this variation is also assumed for the direction of dip of the slope. It should be noted that this assumption is made for major instabilities based on experience and may not be valid for smaller instabilities involving sets of minor discontinuities;
d. The line of intersection must occur below elevation 1400 ft, which is about 100 ft (30 m) above the crest of the pit, and must be above elevation 191 which is about 300 ft (100 m) below the proposed base of the pit; in both cases these elevations and pit geometry are based on the proposed final pit design as of September 1973.

68. The major structures were grouped in areas in which the trend of the bench faces are approximately similar and plotted on equal area nets. Each plot was examined individually and in combination with adjacent equal area nets to define the lines of intersection of all possible unstable wedges using the criteria described above. All intersections falling within the shaded area marked by heavy lines on Fig 15 were

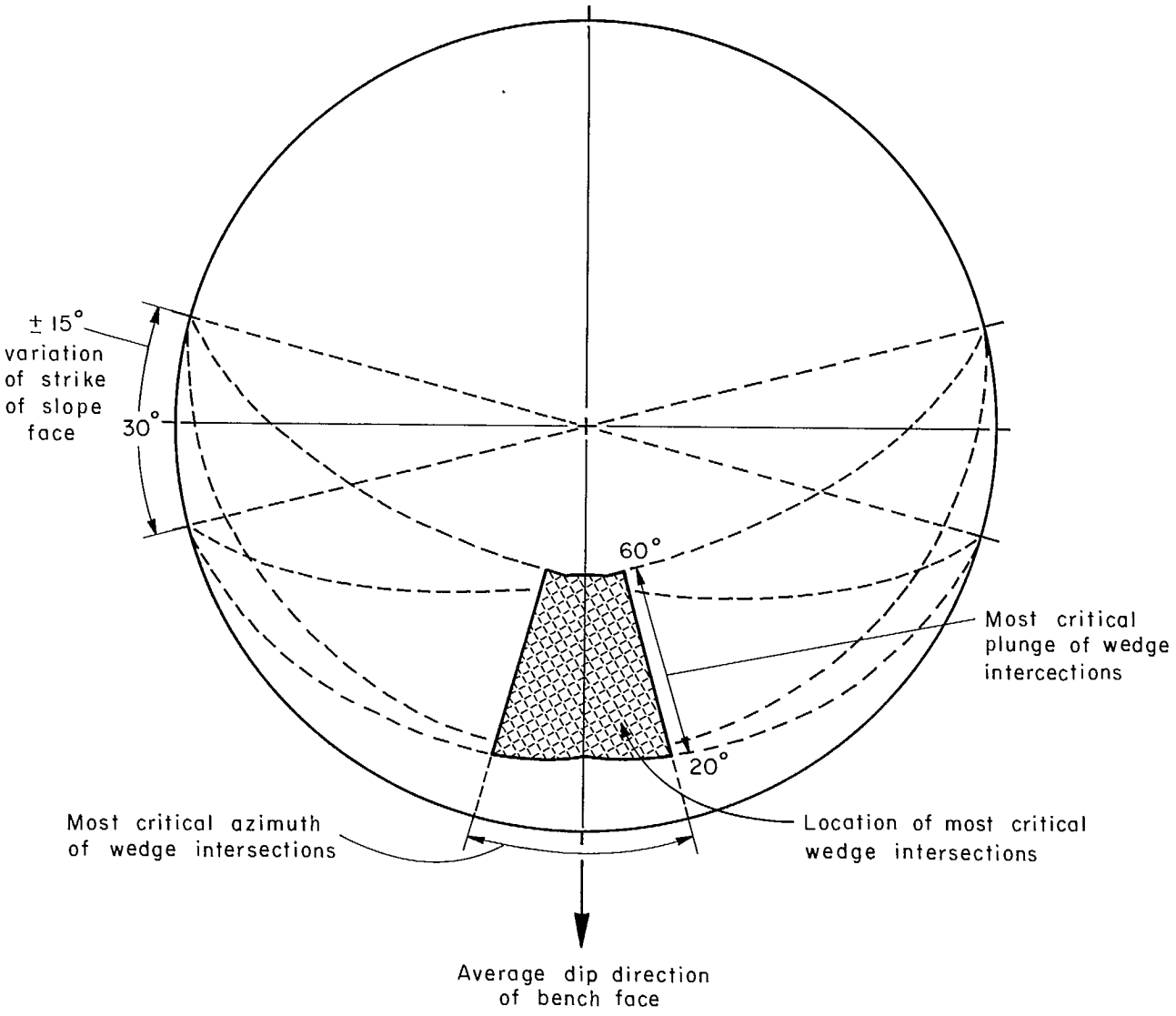

Fig 15 - Critical wedge intersections.

considered unstable wedges.

69. Having defined these wedges, the relationship of the pit geometry and the lines of intersection were examined in plan and section to determine whether the wedges could lead to instability. A list of potentially unstable major wedges and their volumes is given in Table 6. A plot of major faults and unstable wedge intersections is also given in Fig 16.

70. The analysis of major structures indicates seven possible unstable wedges in the pit. Two of these major wedges have already daylighted on the pit slope, but in neither case is any movement indicating critical instability. Wedge 60 + 61 in the footwall has been exposed for over five years and wedge 14 + 24 has been exposed for less than one year in the hanging wall.

71. The lines of intersection of the wedges in the hanging wall plunge at only moderate angles. One of these, ie, 14 + 28, occurs below the proposed pit bottom and the other, 14 + 24, has already been exposed, as explained earlier and has not failed. Of the five wedges on the footwall side of the pit, three have lines of intersection

Table 6: Possible unstable wedges involving major geologic structures

	Structure A				Structure B				Wedge intersection						Bench orientation	Location
	No.	Type	Avg Strike	Avg Dip	No.	Type	Avg Strike	Avg Dip	PL	AZ	Int. Angle	Elev	Easting	Northing	Dip dir	
1	14	FL	027	58E	24	FL	009	90	36	198	34	659	-196.0	374.0	171	HW
2	14	FL	027	58E	28	FL	003	79W	22	188	52	530	- 41.0	288.5	187	HW
3	53	FL	016	73W	63	JN	166	67E	34	004	50	<491 >191	-	-	347	FW
4	45	FL	019	88E	61	FL	176	65E	42	021	32	<491 >191	-	-	343	FW
5	60	JN	019	86E	61	FL	176	65E	44	024	32	1154	+192.0	-541.0	17	FW
6	60	JN	019	86E	63	JN	166	67E	56	026	39	<491 >191	-	-	19	FW
7	63	JN	166	67E	65	FL	018	71W	35	004	52	-	-	-	17	FW

NOTES:
1. PL, AZ and Int angle refer to the plunge and azimuth of the line of intersection and the interior angle of the wedge respectively, FL = Fault, JN = Joint.
2. ELEV, Easting and Northing refer to the elevation and location of the line of intersection of the wedge with the existing or proposed pit wall according to the pit design of September 1973, except where the line of intersection is below the pit face (ie, < 491 and > 191) or where no intersection was observed on the face.
3. Dip dir bench is the average azimuth in degrees of the bench dip direction in the vicinity of the intersection of the line of intersection of the wedge with the existing or proposed pit wall as of September 1973.
4. HW = hanging wall and FW = footwall.

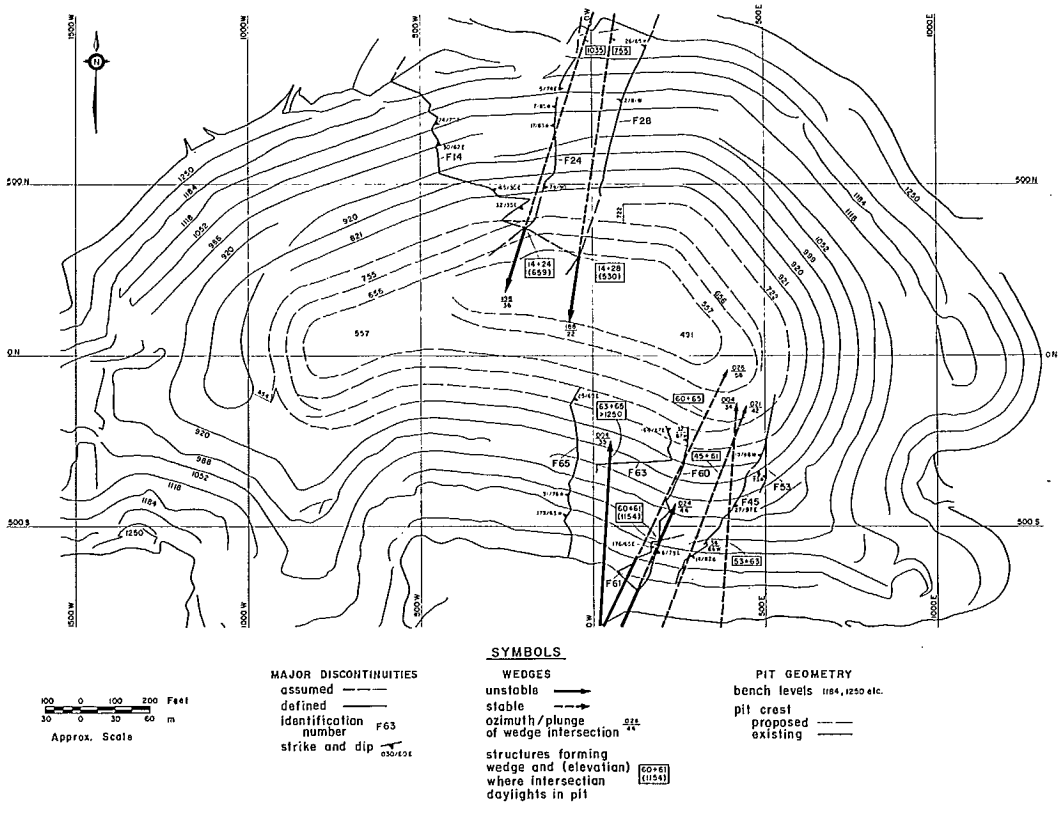

Fig 16 - Critical wedges from fault intersections in proposed slopes of Hilton Mine pit.

Table 7 continued:

IV	East wall	D3	298°	Wedge failure involving set A and set C	6° - 21°	Safe - shallow plunge	None
				Blockflow involving set B	80° - 88° in slope	Safe if not disturbed; small size	Scale benches, controlled blasting, possible use of inclined bench faces
				Blockflow involving set D	62° - 65° in slope	Safe if not disturbed	None
				Wedge failure involving set B and Fault No. 48*	60°	Small	None
				Wedge failure involving set C and Faults No. 46, 50 and 52*	22° - 26°	Safe if dry	Possibly drainholes
V	East footwall	D4	016°	Plane failure on set A with separation on set B	40° - 65	Generally small failures	Use of inclined bench faces
				Wedge failure involving set A and set B	38° - 64°		
				Wedge failures involving set A and set C	40° - 8°	Safe shallow plunge	None
				Wedge failures involving set A and set D	39° - 62°	Critical	Shear strength investigation; possible artificial support and drainage in critical areas
				Wedge failure involving set A and north-south striking faults	39° - 61°	Critical	Artificial support in critical areas
				Wedge failures involving set B and north-south striking faults	35° - 60°	Small dihedral angle	None
				Wedges involving set D and Faults No. 45 and 60	53° & 58°	Small dihedral angle	None
VI	Sothwest nose nose	D4+D5	324°	Plane failure on set A with separation on set B	40° - 65°	Generally small	Use of inclined bench faces
				Wedge failures involving set A and set B	37° - 39°	Generally small	
				Wedge failures involving set C	4° - 12°	Safe - shallow	None
				Wedge failures involving set D	42° - 62°	Critical	Shear strength investigation; possible artificial support and drainage in critical areas
				Wedge failures involving set A and Fault No. 68*	51°	Critical	Artificial support where required
				Wedges involving sets B or D and	20° - 60° Major faults	Small dihedral angle	None
VII	West footwall	D5	025°	Plane failure on set A with separation on set B	56°	Small failures	Use of inclined bench faces
				Wedge failures involving set A and set B	59°	Small failures	
				Wedge failures involving set A and set D	50°	Small failures	Use of inclined bench faces; possibly some artificial support
				Wedges involving set A and Faults No. 71 and 73*	32° & 60°	Critical	Artificial support where required
				Wedges involving set B or D and Major faults	22° - 60°	Small dihedral angle	None

*Faults are not shown in Fig 1 or 16. Details are given below:

Fault No.	Strike/dip	Mid point	Length (ft)	Fault No.	Strike/dip	Mid point	Length (ft)
46	085/13BS	673E/060N	100	68	010/80W	356W/200S	105
48	016/85W	767E/011S	220	71	015/85W	791W/800S	180
50	090/45N	1111E/200S	135	73	030/90	962W/450S	100
52	095/55N	684E/344S	100				

procedures and remedial work. Since the size of minor discontinuities relative to faults is considerably less in most cases, any of the postulated possible wedge failures to be discussed in the following paragraphs are likely to be small in size, less than one bench, and of a local nature only.

Hanging Wall (Design Sectors I, II and III)

87. The dominant north-south striking set of faults form possible wedges with set C virtually at all locations where these faults exist on the hanging wall. As indicated in Table 7 the lines of intersection of these wedges plunge between 20° and 40° towards the pit.

88. Examples of wedge failures involving set C are especially apparent in the hanging wall area shotcreted in July 1973. Wedge failures involving set C and the Southwest Fault have caused unravelling and narrowing of the haul road at this point. Table 7 indicates that this is not unique and possible wedge failures exist wherever easterly dipping major faults cross the hanging wall side of the pit. This implies that further remedial measures may be required where the haul road crosses the Central Fault Zone at lower levels. The likelihood of wedge instability may be reduced if the frequency of set C decreases with depth.

89. Wedges formed from combinations of the steeply dipping cross fracture set B occur only with faults no. 24 and 28 in design sector II. The wedges formed by these sets have a very small dihedral angle and the discontinuous nature of set B, tend to make large wedge failures unlikely.

90. Also, wedges are formed by combining joint set D with faults no. 24 and 28. No failures, however, have been observed involving these features in the pit.

East Wall (Design Sector IV)

91. On the east wall, set C forms shallow dipping wedges with faults no. 46, 50 and 52. Failures involving these features were not noted in the pit, possibly because the major structures involved are not well defined, possibly because they occur in areas of shallow slope; or possibly because they are only partly exposed. The steeply dipping cross fractures ie, set B, also form wedges with faults no. 46 and 48. The discontinuous nature of set B probably explains why wedge failures are not seen on the east wall.

Footwall (Design Sectors V, VI and VII)

92. On the footwall side of the pit, set C dips into the wall. Set A on the other hand, dips parallel to the wall, leading to plane shear failures, and in combination with transverse faults form unfavourable steeply dipping wedges.

93. The cross fractures of set B form wedges with north-south trending faults in the footwall. However, because of possible variation in the strike and dip of the fractures, possible wedges are small and tend to have very small dihedral angles.

94. Set D could also form wedges with some westerly dipping or vertical structures on the footwall, such as faults no. 45, 60, 28, 65, 68, 71 and 73.

CONTACTS OF INTRUSIVES

95. Contacts of intrusive rocks such as granite and granodiorite appear to have a well developed north-south trend and 30° to 60° westerly dip in the pit area. These structures could lead to plane shear instability if they persist in the east wall in design sector IV.

96. Since these features are nearly parallel to the dominant set of transverse faults, their line of intersection with these faults is flat lying and therefore of little consequence on the hanging wall. However, on the footwall side in design sectors V, VI and VII, geological contacts in combination with set A and compositional layering parallel to set A have led to occasional wedge failures.

THE SOUTHWEST NOSE AREA

97. The southwest nose in design sector VI on the footwall side immediately east of the sump, consists largely of intrusive waste rock in the upper parts of the slope. The slope configuration on the southwest nose is highly conducive to instability because it has a reverse radius of

curvature, ie, the slope is convex outwards instead of concave inwards. It is understood that three moderate size failures have occurred in this section of the footwall.

98. A recent failure on bench 920S involved the Southwest fault and several major joints and shears which form a zone of large loose blocks in the slope (Fig 20). Material fell from this zone twice during the summer of 1973 and loose material still exists. Groundwater along the Southwest fault appears to have contributed to the failures.

99. The Southwest fault has a well brecciated zone on the lower part of the footwall and flattens considerably with depth. The intersection of the Southwest fault and the Observation fault is visible on bench 799S (Fig 20) but dips into the face and does not present any potential stability problem. However, several other faults on the Southwest nose could be involved in possible instability.

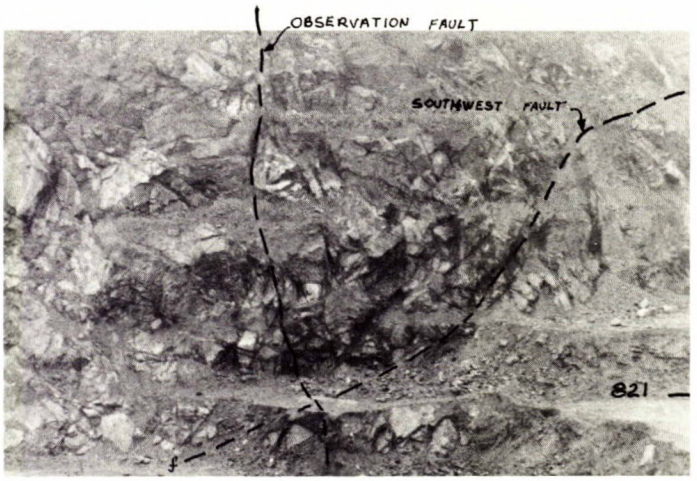

Fig 20 - Unstable southwest nose area due to intersection of observation fault and southwest fault (F 13).

REFERENCES

1. Sabourin, J.E. "Bristol-Masham area, Pontiac and Gatineau Counties, Quebec"; Department of Natural Resources; Geological Report no. 110, pp 44; 1965.

Table 7 continued:

IV	East wall	D3	298°	Wedge failure involving set A and set C	6° - 21°	Safe - shallow plunge	None
				Blockflow involving set B	80° - 88° in slope	Safe if not disturbed; small size	Scale benches, controlled blasting, possible use of inclined bench faces
				Blockflow involving set D	62° - 65° in slope	Safe if not disturbed	None
				Wedge failure involving set B and Fault No. 48*	60°	Small	None
				Wedge failure involving set C and Faults No. 46, 50 and 52*	22° - 26°	Safe if dry	Possibly drainholes
V	East footwall	D4	016°	Plane failure on set A with separation on set B	40° - 65	Generally small failures	Use of inclined bench faces
				Wedge failure involving set A and set B	38° - 64°		
				Wedge failures involving set A and set C	40° - 8°	Safe shallow plunge	None
				Wedge failures involving set A and set D	39° - 62°	Critical	Shear strength investigation; possible artificial support and drainage in critical areas
				Wedge failure involving set A and north-south striking faults	39° - 61°	Critical	Artificial support in critical areas
				Wedge failures involving set B and north-south striking faults	35° - 60°	Small dihedral angle	None
				Wedges involving set D and Faults No. 45 and 60	53° & 58°	Small dihedral angle	None
VI	Sothwest nose nose	D4+D5	324°	Plane failure on set A with separation on set B	40° - 65°	Generally small	Use of inclined bench faces
				Wedge failures involving set A and set B	37° - 39°	Generally small	
				Wedge failures involving set C	4° - 12°	Safe - shallow	None
				Wedge failures involving set D	42° - 62°	Critical	Shear strength investigation; possible artificial support and drainage in critical areas
				Wedge failures involving set A and Fault No. 68*	51°	Critical	Artificial support where required
				Wedges involving sets B or D and	20° - 60° Major faults	Small dihedral angle	None
VII	West footwall	D5	025°	Plane failure on set A with separation on set B	56°	Small failures	Use of inclined bench faces
				Wedge failures involving set A and set 8	59°	Small failures	
				Wedge failures involving set A and set D	50°	Small failures	Use of inclined bench faces; possibly some artificial support
				Wedges involving set A and Faults No. 71 and 73*	32° & 60°	Critical	Artificial support where required
				Wedges involving set B or D and Major faults	22° - 60°	Small dihedral angle	None

*Faults are not shown in Fig 1 or 16. Details are given below:

Fault No.	Strike/dip	Mid point	Length (ft)	Fault No.	Strike/dip	Mid point	Length (ft)
46	085/138S	673E/060N	100	68	010/80W	356W/200S	105
48	016/85W	767E/011S	220	71	015/85W	791W/800S	180
50	090/45N	1111E/200S	135	73	030/90	962W/450S	100
52	095/55N	684E/344S	100				

procedures and remedial work. Since the size of minor discontinuities relative to faults is considerably less in most cases, any of the postulated possible wedge failures to be discussed in the following paragraphs are likely to be small in size, less than one bench, and of a local nature only.

Hanging Wall (Design Sectors I, II and III)

87. The dominant north-south striking set of faults form possible wedges with set C virtually at all locations where these faults exist on the hanging wall. As indicated in Table 7 the lines of intersection of these wedges plunge between 20° and 40° towards the pit.

88. Examples of wedge failures involving set C are especially apparent in the hanging wall area shotcreted in July 1973. Wedge failures involving set C and the Southwest Fault have caused unravelling and narrowing of the haul road at this point. Table 7 indicates that this is not unique and possible wedge failures exist wherever easterly dipping major faults cross the hanging wall side of the pit. This implies that further remedial measures may be required where the haul road crosses the Central Fault Zone at lower levels. The likelihood of wedge instability may be reduced if the frequency of set C decreases with depth.

89. Wedges formed from combinations of the steeply dipping cross fracture set B occur only with faults no. 24 and 28 in design sector II. The wedges formed by these sets have a very small dihedral angle and the discontinuous nature of set B, tend to make large wedge failures unlikely.

90. Also, wedges are formed by combining joint set D with faults no. 24 and 28. No failures, however, have been observed involving these features in the pit.

East Wall (Design Sector IV)

91. On the east wall, set C forms shallow dipping wedges with faults no. 46, 50 and 52. Failures involving these features were not noted in the pit, possibly because the major structures involved are not well defined, possibly because they occur in areas of shallow slope; or possibly because they are only partly exposed. The steeply dipping cross fractures ie, set B, also form wedges with faults no. 46 and 48. The discontinuous nature of set B probably explains why wedge failures are not seen on the east wall.

Footwall (Design Sectors V, VI and VII)

92. On the footwall side of the pit, set C dips into the wall. Set A on the other hand, dips parallel to the wall, leading to plane shear failures, and in combination with transverse faults form unfavourable steeply dipping wedges.

93. The cross fractures of set B form wedges with north-south trending faults in the footwall. However, because of possible variation in the strike and dip of the fractures, possible wedges are small and tend to have very small dihedral angles.

94. Set D could also form wedges with some westerly dipping or vertical structures on the footwall, such as faults no. 45, 60, 28, 65, 68, 71 and 73.

CONTACTS OF INTRUSIVES

95. Contacts of intrusive rocks such as granite and granodiorite appear to have a well developed north-south trend and 30° to 60° westerly dip in the pit area. These structures could lead to plane shear instability if they persist in the east wall in design sector IV.

96. Since these features are nearly parallel to the dominant set of transverse faults, their line of intersection with these faults is flat lying and therefore of little consequence on the hanging wall. However, on the footwall side in design sectors V, VI and VII, geological contacts in combination with set A and compositional layering parallel to set A have led to occasional wedge failures.

THE SOUTHWEST NOSE AREA

97. The southwest nose in design sector VI on the footwall side immediately east of the sump, consists largely of intrusive waste rock in the upper parts of the slope. The slope configuration on the southwest nose is highly conducive to instability because it has a reverse radius of

curvature, ie, the slope is convex outwards instead of concave inwards. It is understood that three moderate size failures have occurred in this section of the footwall.

98. A recent failure on bench 920S involved the Southwest fault and several major joints and shears which form a zone of large loose blocks in the slope (Fig 20). Material fell from this zone twice during the summer of 1973 and loose material still exists. Groundwater along the Southwest fault appears to have contributed to the failures.

99. The Southwest fault has a well brecciated zone on the lower part of the footwall and flattens considerably with depth. The intersection of the Southwest fault and the Observation fault is visible on bench 799S (Fig 20) but dips into the face and does not present any potential stability problem. However, several other faults on the Southwest nose could be involved in possible instability.

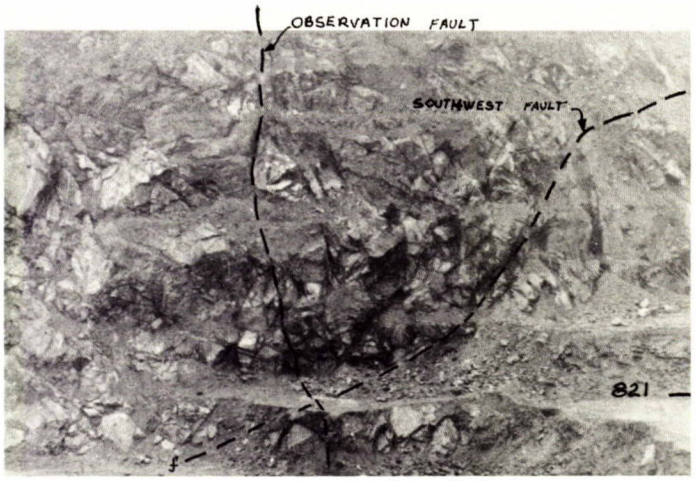

Fig 20 - Unstable southwest nose area due to intersection of observation fault and southwest fault (F 13).

REFERENCES

1. Sabourin, J.E. "Bristol-Masham area, Pontiac and Gatineau Counties, Quebec"; Department of Natural Resources; Geological Report no. 110, pp 44; 1965.